

# An Optimized Micromixer with Patterned Grooves

Yanghua Tang, Jonathan Wu, Eva Czyzewska, Kevin Stanley  
Institute for Fuel Cell Innovation, National research Council, Canada  
Yanghua.tang@nrc-cnrc.gc.ca

## Abstract

With the development of microfluidic systems, there is a growing interest in micro scale laminar flow mixing. In this work, the fluid rotating angle and mixing efficiency in a micromixer with patterned grooves are studied as a function of the dimensions of the microstructure by numerical simulation. We found that mixing efficiency does not always increase with higher fluid stream rotation in the microchannel. High groove aspect ratios are not advantageous to fluid rotation. Experiments on mixture of two fluids were done on a micromixer fabricated in PDMS by replica molding. An 85% mixing efficiency was obtained in a 30mm long mixing channel with two dyed liquids.

## 1. Introduction

Rapid mixing is increasingly important in many of microfluidic applications, such as lab-on-a-chip chemical analysis, PCR amplification and micro fuel cells. Fluid mixing can be achieved by convection or diffusion. In a typical microfluidic device, the Reynolds number is low and flow is laminar. Mixing is achieved only by molecular diffusion, which is a much slower process than convection. In molecular diffusion, the volume mixed  $V$  at a given time  $t$  is

$$V = A\sqrt{Dt} \quad (1)$$

Where  $A$  is the contact area between the fluids and  $D$  is diffusion constant. This equation shows that an efficient way to speed up the molecular diffusion is to increase the contact area of fluids.

Two methods can be used to improve mixing efficiency in microfluidic devices. One method requires inducing turbulent flow, causing convective mixing. Active parts can be integrated in the micro devices to perturb flow, such as the 25 $\mu$ m-high magnetic microstirrer array integrated in the flow field [1]. However, integration of moving parts in the mixers leads to the difficulty in microdevice fabrication. Turbulent flow can also be caused by putting obstacles into the flow

field [2]. However, pressure losses increase because of turbulent flow in the channel.

Another method to increase mixing speed is to increase the contact area between fluids by splitting, folding and stretching laminar flows in the microchannels. Some microstructures are designed to split and twist fluid streams at low  $Re$ , such as multi-layer and multi-stage mixers [3,4]. It is not easy to manufacture these microstructures because the common lithographic methods used in microfabrication lead to planar, layered structures. One simple microstructure, which can stretch and fold flows, is a microchannel with patterned grooves which has been studied by several research groups [5-8]. Helical flow can be created in the microchannel with patterned grooves over a wide  $Re$  range and efficient mixing can be obtained in a short distance.

In this work, numerical simulation was performed to investigate the relationship between the dimensions of a patterned-groove micromixer and fluid rotation in the micromixer. Mixing efficiency was also estimated. Mixing experiments were done in a micromixer designed according to the simulation results.

## 2. Numerical simulation

### 2.1. Simulation setup

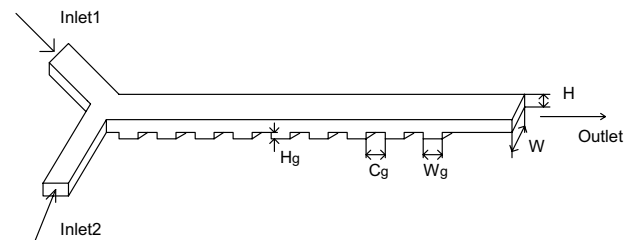


**Figure 1. Micromixer with patterned grooves, the angle between channel and grooves is 45°. The groove width  $W_g$  is equal to the distance  $C_g$  between adjacent grooves. The period of grooves  $Q$  is  $W_g + C_g$ .**

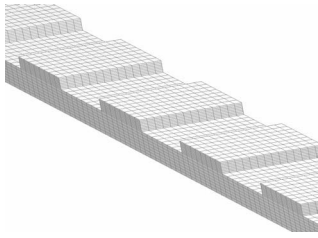


**Figure 2. Meshed channel and grooves**

The structure of the micromixer is shown in figure 1. Computational fluid dynamics software (CFD), CFD-ACE 2003, was used to calculate the 3D velocity field as well as two-fluid mixing. Structured meshes were built by CFD-GEOM to generate a stable solution, as shown in figure 2. The quality of the meshes was examined and modified to speed up convergence and achieve accurate simulation results.

In CFD-ACE 2003, the flow module and the user scalar module were used to solve the Navier Stokes equation and mass transport equation. Simulations were run as steady, laminar, and Newtonian. Both inlets were assigned the same flow rate. Flow velocities ranged from 5mm/s to 50mm/s. The inlets were set to pure concentrations of fluid1 and fluid2. The diffusion coefficient,  $D$ , was  $1.26 \times 10^{-5} \text{ cm}^2 \text{ s}^{-1}$ . The length of the mixing channels was 10mm. The width and depth of the channel were varied respectively from  $100\mu\text{m}$  to  $600\mu\text{m}$  and from  $100\mu\text{m}$  to  $400\mu\text{m}$ . The width and depth of the grooves were varied from  $50\mu\text{m}$  to  $400\mu\text{m}$  and from  $50\mu\text{m}$  to  $400\mu\text{m}$  respectively.

**2.2. Simulation results and discussion**

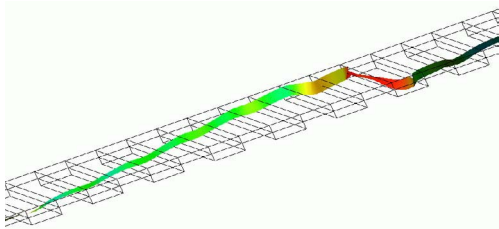


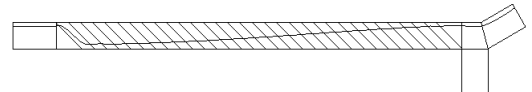
**Figure 3. Stretched and folded fluid streams in the channel with patterned grooves**



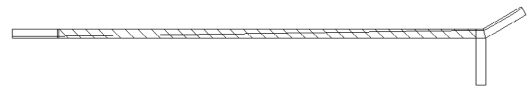
**Figure 4. The fraction distribution of fluid2 from inlet2**

Simulation shows that two fluids in the channel are stretched and folded, and therefore, the interfacial area

between two fluids in the mixing channel is increased. The helical fluid streams in the channels are shown in Figure 3. The twisted fluid streams are made by the anisotropic shear stress in the channel which is caused by the patterned grooves at the channel bottom. The stretching and folding of volumes of the fluid proceed exponentially as a function of the axial distance traveled by the volume [6]. Therefore, rapid mixing can be achieved. The distribution of the fluid2 fraction in the mixing channel is shown in Figure 4. The green area (or the gray area in black-white print) indicates where two fluids are mixed.



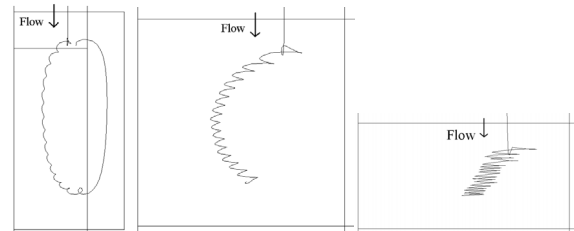
**a1  $\alpha = 2.87^\circ$**



**b1  $\alpha = 0.84^\circ$**



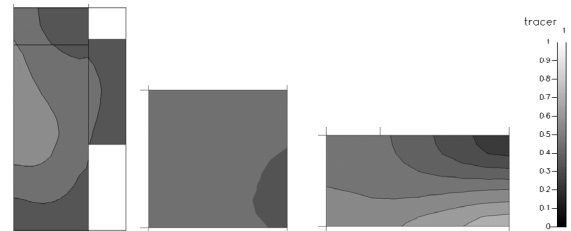
**c1  $\alpha = 0.27^\circ$**



**a2**

**b2**

**c2**



**a3  $M = 0.85$**

**b3  $M = 0.94$**

**c3  $M = 0.81$**

**d**

**Figure 5. Fluid2 fraction distributions in the cross section of the mixing channel. The channel depth  $H$  is  $200\mu\text{m}$ . (a1, a2, a3)  $W = 600\mu\text{m}$ , (b1, b2, b3)  $W = 200\mu\text{m}$ , (c1, c2, c3)  $W = 100\mu\text{m}$ .**

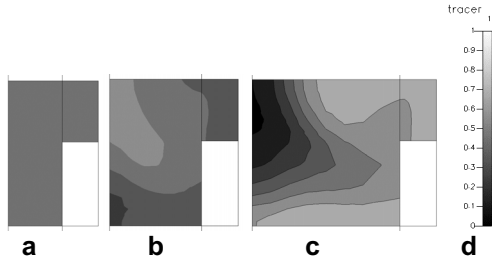


**Figure 6. Fluid2 fraction distributions in the cross section of the mixing channel. The channel width  $W$  is  $400\mu\text{m}$ . (a)  $H = 150\mu\text{m}$ ,  $\alpha = 3.67^\circ$ ,  $M = 0.99$  (b)  $H = 250\mu\text{m}$ ,  $\alpha = 1.59^\circ$ ,  $M = 0.84$  (c)  $H = 400\mu\text{m}$ ,  $\alpha = 0.47^\circ$   $M = 0.65$**

The rotation effect of fluids can be estimated by the angle  $\alpha$  between the channel axis and interfacial surface of two fluids. To evaluate the mixing efficiency in the mixing channel, the mixing index  $M$  is defined as follows:

$$M = 1 - \sqrt{\frac{1}{\sum A_i} \sum (c_i - \bar{c})^2 A_i} \quad (2)$$

where  $A_i$ ,  $c_i$  and  $\bar{c}$  are the  $i^{\text{th}}$  element area, the fluid2 fraction of the  $i^{\text{th}}$  element and the fluid2 mean fraction (area weight) in the certain cross section of the mixing channel respectively. In the following simulation, the mixing index is calculated in the 9 mm long mixing channel.

To visualize the fluid streams, non-diffusive particle traces can be implemented numerically approach in CFDRC, as shown in figure 5a1, 5b1, and 5c1. It shows that the rotating angle of fluid streams in the microchannel increases with the channel width. To show fluid stream twisting clearly in the mixing channel, the particle traces in the figure 5a1, 5b1 and 5c1 are projected to the cross section in the mixing channels, as shown figure 5a2, 5b2, and 5c2. The flows twist more in the shallower channel. When  $\alpha = 2.87$ , one circulation is complete in the mixing channel. Intriguingly, the change of mixing index  $M$  is not consistent with that of rotating angle. The fluid2 fraction distribution in the cross section of the mixing channel is shown in figure 5a3, 5b3, 5c3. At a channel width of  $600\mu\text{m}$ , the mixing index decreases to 0.85. Although the stronger rotation of fluid streams in the channel is advantageous to mixing, the wider channel leads to a longer diffusion distance along which the main diffusing process proceeds. Thus, wider channels are beneficial to fluid rotation, but not always to mixing process. In figure 6, the rotation angle of fluid streams and the mixing index decreases with rising of the channel depth.

From figure 5 and figure 6, we can deduce that the effect of channel width on mixing index is different from

that of channel depth the channel although the same aspect ratio can be achieved by changing the channel width or depth. The variation of the channel width affects not only the diffusing distance of two fluids in the channel, but also groove length while variation of the channel depth does not affect the groove dimension. Longer diffusing distances impair the mixing efficiency, but long grooves make fluid stream rotate more strongly and improve the mixing efficiency.

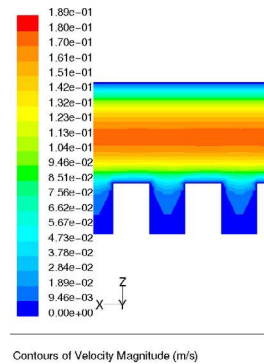


**Figure 7. Velocity field in the grooves**

Simulation shows that the rotating angle  $\alpha$  and mixing index  $M$  increase with deeper grooves. But at a groove ratio aspect of more than 1.5, the change of rotating angle  $\alpha$  and mixing index  $M$  is small. The higher aspect ratio creates stagnant zones in the groove, as shown in Figure 7 and decreases the effect of grooves on the transverse stress in the channel.

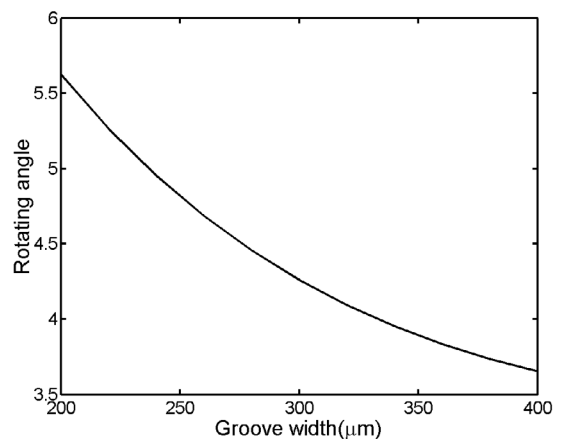


**Figure 8. Rotating angle versus groove width. Channel depth  $H$  is  $200\mu\text{m}$ , and groove depth  $H_g$  is  $50\mu\text{m}$ .**

When the angle between the grooves and the mixing channel is  $45^\circ$ , rotating angle can be estimated theoretically [9].

$$\tan(\alpha) = \frac{a^2(k_1(U) - k_2(U))}{2 - a^2(3 - k_1(U) - k_2(U))} \quad (4)$$

Where the micromixer dimensional parameters are  $a = H_g / (H_g + H)$  and  $U = 2\pi H / Q$ .  $k_1$  and  $k_2$  are the functions of  $U$

$$k_1(U) = -1 + 2U \frac{\sinh(U)\cosh(U) - U}{\sinh^2(U) - U^2} \quad (5)$$

$$k_2(qH) = -1 + U \frac{\cosh(U)}{\sinh(U)} \quad (6)$$

Equation 4 is valid in the combined limit of  $a \ll 1$  and  $a*U \ll 1$ . It shows in figure 8 that rotating angle decreases with wider grooves. This effect is also demonstrated by numerical simulation. Too narrow grooves negatively affect the rotation angle and mixing efficiency, as shown in figure 9. When the grooves reach  $50 \mu\text{m}$ , the rotation angle is only  $0.67^\circ$ . The groove width affects not only the groove aspect ratio, but also the groove period  $Q$ . It can be concluded that too short or too long groove period weakens the fluid rotation, and decreases the mixing efficiency.

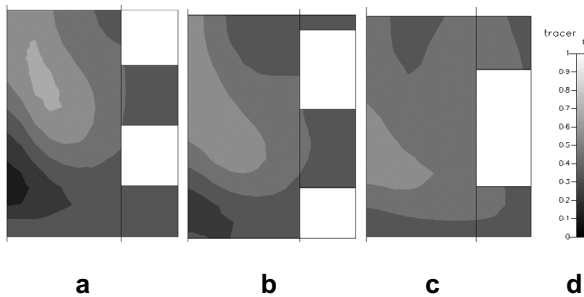


**Figure 9. Fluid2 fraction distributions in the cross section of the mixing channel. The groove depth  $H_g$  is  $100 \mu\text{m}$  (a)  $W_g = 50 \mu\text{m}$ ,  $\alpha = 0.67^\circ$ ,  $M = 0.75$  (b)  $W_g = 100 \mu\text{m}$ ,  $\alpha = 1.94^\circ$ ,  $M = 0.80$  (c)  $W_g = 150 \mu\text{m}$ ,  $\alpha = 2.18^\circ$ ,  $M = 0.90$ .**

According to our simulation results, the effect of the width of the channels and grooves on the rotation angle of fluid streams in the channel is not the same as that of the depth of channel and grooves, although the same channel or groove aspect ratio can be made by changing channel or groove width or depth. The results on the relationship among fluid rotation, mixing and dimension of microstructure was used to design a micromixer with patterned grooves.

### 3. Micromixer and experiments

Micromixers with patterned grooves have been designed based on the simulation results. The channel width and depth were  $600 \mu\text{m}$ ,  $200 \mu\text{m}$  respectively. Although such a wide channel is not good for mixing,

distinct rotation of fluid streams can be observed in the mixing channel. The groove width and depth are  $200 \mu\text{m}$  and  $225 \mu\text{m}$  respectively. A total of 56 grooves were fabricated in the  $30\text{mm}$ -long mixing channel.

### 3.1 Fabrication of the micromixer

The micromixer was made in Polydimethyl siloxane (PDMS) by replica molding, as shown figure 10. The master was made from SU-8 on a silicon substrate. The PDMS was cured in the oven of  $75^\circ\text{C}$  for 1.5 hours, and then the PDMS replica was peeled from the master. The cured PDMS was aligned and bonded to a glass slide with access holes for channels and reservoirs. The bonding of PDMS and glass is reversible. PDMS can be exposed to an  $\text{O}_2$  plasma to obtain irreversible bonding [10].

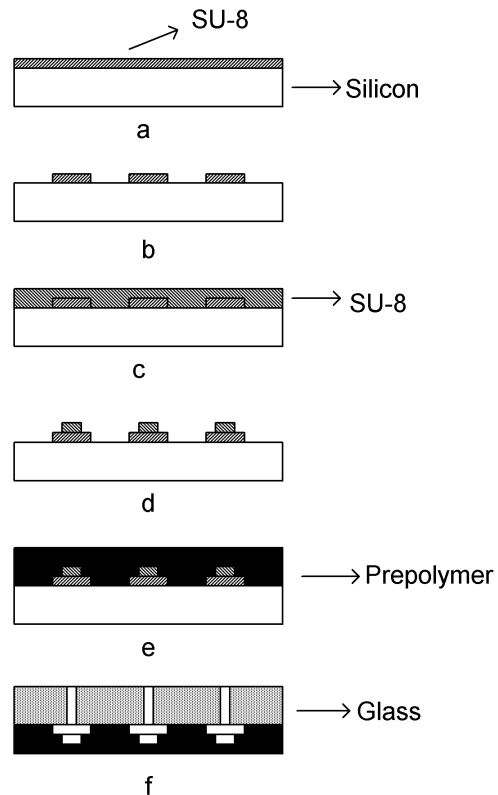


**Figure 10. Fabrication process of replica molding of micromixer. (a) The first SU-8 layer is coated on the silicon substrate. (b) The channel pattern is transferred to SU-8. (c) The second SU-8 layer is coated on the silicon substrate. (d) The groove pattern is transferred to the second SU-8 layer. (e) Prepolymer is cast to the SU-8 mold. (f) Cured PDMS is bonded to glass.**

### 3.2. Mixing experiments

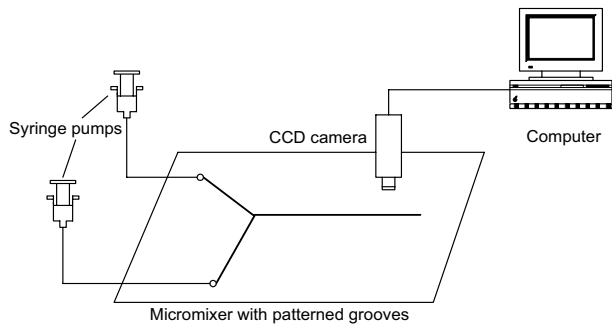
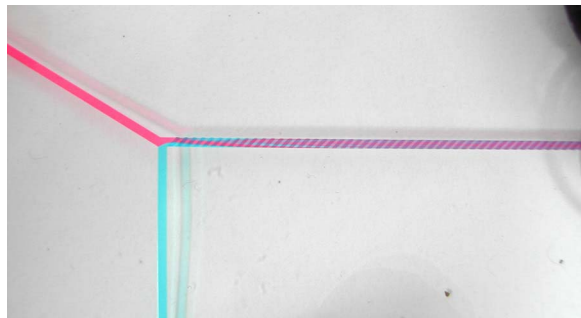
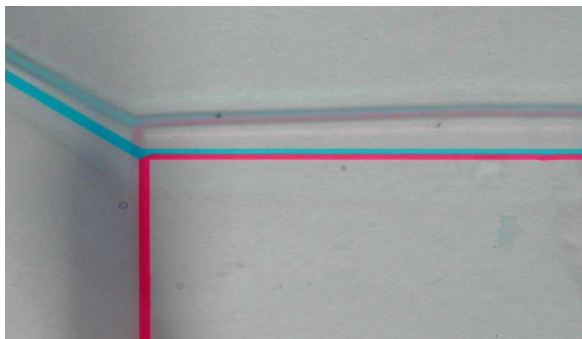


**Figure 11. Schematic setup for mixing experiments**



**a**



**b**

**Figure 12. Rotation and mixing of two colored fluids**

The mixing experiment setup is schematically shown in Figure 11. The fluid was pumped into the channels by pressure-driven syringes. The flow rate was approximately 0.3ml/min. Mixing can be visualized by using fluorescent dye, pH indicators and colored dyes. In this paper, red and blue dyed water were injected into the micromixer to make the mixing process visible. A CCD camera was used to capture the mixing. The resulting 24-bit colored image was analyzed by the image processing software (Scion Image) and the color index was calculated in every pixel [1]. Similar to the definition of

mixing index in the simulation, the mixing index which is used to express the efficiency at a given cross section in the mixing channel is defined as follows:

$$\text{mixing index} = 1 - \sqrt{\frac{1}{N} \sum \left( \frac{I_k - \bar{I}}{\bar{I}} \right)^2} \quad (7)$$

where  $N$  is pixel amount in the cross section,  $I_k$  is the color index at the pixel  $k$  and  $\bar{I}$  is the mean value of color index over the  $N$  pixels.

The mixing of two colored fluids is shown in figure 12. The red and blue water were injected into the two inlets at the same flow rate. In the channel with patterned grooves, fluid stream twisting appeared, as shown in figure 12a. If there is no groove in the mixing channel, the stable interfacial line appears in the middle for the entire mixing channel, as shown figure 12b. At the end of the channel with patterned grooves, the interfacial line disappeared and the two fluids were well mixed. The mixing index in the 3cm-long mixing channel was estimated as 85%.

#### 4. Conclusions

In this paper, fluid rotation and mixing in channels with patterned grooves was studied in the laminar flow regime by numerical simulations and experiments. The effect of dimensions of channels and grooves on the rotation angle and mixing efficiency was investigated. Stronger rotation can be reached in shallower channels. But mixing index does not always increase with wider channel because of longer diffusing distance. High groove aspect ratios (but less than 1.5) are beneficial to mixing. Too narrow or too wide groove impairs mixing the efficiency. The simulation results provide guidance to optimizing the design of the micromixer. The micromixer was designed according to the simulation results and fabricated in PDMS with replica molding. Mixing experiments shows an 85% mixing index can be achieved in 30mm-long mixing channel with two dyed liquids.

#### Reference

- [1] Liang-Hsuan Lu, Kee Suk Ryu, and Chang Liu, "A magnetic microstirrer and array for microfluidic mixing", *J. Microelectromech. Syst.*, Vol.11, 2002, pp. 462-469.
- [2] Zuomin Dong, Ken W. Kratschma, Dongming Lu, Ryan N. Mackie, Walter R. Merida Donis, Michael E. Pastula, Martin L. Perry, Gaofeng Gary Wang, Rong Zheng, "Oxidant flow field for solid polymer electrolyte fuel cell", *US Patent*: 0119360, 2002.
- [3] Robin H.Liu, Mark A. Stremmer, Kendra V. Sharp, Michael G. Olsen, Juan G. Santiago, Ronald J. Adrian, "Passive mixing in a three-dimensional serpentine microchannel", *J. Microelectromech. Syst.*, Vol. 9, 2000, pp. 190-197.

- [4] Sung-Jin Park, Jung Kyung Kim, Junba Park, Seok Chung, Chanil Chung and Keun Chang, "Rapid three-dimensional passive rotation micromixer using the breakup process", *J. Micromech. Microeng.* Vol. 12, 2004, pp. 6-14.
- [5] Timothy J. Johnson, Svid Ross, and Laurie E. Locascio, "Rapid microfluidic mixing", *Anal. Chem.* Vol.74, 2002, pp. 45-51.
- [6] Abraham D. Stroock, Stephan K. W. Dertinger, Armand Ajdari, Igor Mezić, Howard A. Stone, George M. Whitesides, "Chaotic mixer for microchannels", *Science*, Vol. 295, 2002, pp. 647-651.
- [7] Armand Ajdari, "Transverse electrokinetic and microfluidic effects in micropatterned channels: Lubrication analysis for slab geometries", *Physical Review E*, Vol. 65, 2001, 016301.
- [8] Hengzi Wang, Pio Iovenitti, Erol Harvey, Syed Masood, "Numerical Investigation of mixing in microchannels with patterned grooves", *J. Micromech. Microeng.* Vol. 13, 2003, pp. 801-808.
- [9] Abraham D. Stroock, Stephan K. Dertinger, George M. Whitesides, and Armand Ajdari, "Patterning flows using grooved surfaces", *Anal. Chem.* Vol. 74, 2002, pp. 5306-5312.
- [10] Byung-Ho Jo and David J. Beebe, "Fabrication of three-dimensional microfluidic systems by stacking molded polydimethylsiloxane(PDMS) layers", *SPIE*, Vol. 3877, 1999, pp. 222-228.